ISSN 1027-4510, Journal of Surface Investigation. X-ray, Synchrotron and Neutron Techniques, 2015, Vol. 9, No. 5, pp. 1005–1011. © Pleiades Publishing, Ltd., 2015.
Original Russian Text © L. Enkhtor, V.M. Silonov, 2015, published in Poverkhnost'. Rentgenovskie, Sinkhrotronnye i Neitronnye Issledovaniya, 2015, No. 10, pp. 16–22.

Short-Range Order in Solid Solutions of Iron–Rhenium

L. Enkhtor[a] and V. M. Silonov[b]

[a] *Department of Physics, School of Science, National University of Mongolia, Ulaanbaatar, 210646 Mongolia*

[b] *Department of Solid State Physics, Faculty of Physics, Moscow State University, Moscow, 119991 Russia*

e-mail: enkhtor@mail.ru, silonov_v@mail.ru

Received January 20, 2015

Abstract—Using the method of diffuse X-ray scattering, the short-range order parameters for the first four coordination spheres of Fe–Re alloys containing 3, 5, and 7 at % of Re are experimentally determined. These parameters are used to calculate the ordering energy of these alloys within the Cowley approximation. The concentration dependences of the ordering energy and the short-range order parameters for the first four coordination spheres are found. For body-centered cubic superstructures B3, B32, and DO_3, expressions for calculation of the critical temperature of the order–disorder phase transition are derived via the ordering energy. With these expressions, the tendency of Fe–7 at % Re alloy to ordering of the B3 type is revealed.

Keywords: diffuse X-ray scattering, short-range order, ordering energy, Cowley equation, critical temperature of the order–disorder transition

DOI: 10.1134/S1027451015050250

INTRODUCTION

Short-range order and short-range phase separation, as well as long-range order, characterize the fine structure of solid solutions [1–3]. To find their parameters, X-ray and neutron diffraction methods are used. Solid solutions with a face-centered cubic (FCC) lattice are the most studied; a close connection between their fine structure and physical properties has been established. However, there are hardly any studies devoted to investigating short-range order in alloys with a body-centered cubic (BCC) lattice. The existence of short-range order in solid solutions with the BCC structure has been determined by diffuse X-ray scattering only in some binary alloys, for example, Fe–Al [4–8], Fe–3.1 at % Mo [9], Fe–2 at % W [10], Fe–2.5 at % Rh [11], and Fe–5 at % Re [12]. A characteristic feature of the short-range order in Fe–Al alloys is the negative value of its parameters for the first two coordination spheres, indicating short-range order of the Fe_3Al type. In solid solutions of Fe–Mo, negative values of the short-range order parameters appear only starting at the fourteenth coordination sphere. The study of short-range order in alloys of iron with tungsten, rhodium, and rhenium is fragmentary in nature. In BCC alloys, there is a significant size effect, considerably affecting the formation of diffuse scattering. In particular, it may lead to a lack of intense diffuse maxima discernible in the presence of short-range order. The procedure applied in this paper accounts for the size effect more precisely than in early radiographic studies and thus improves the accuracy of determining the short-range order parameters. Determination of the ordering energy by means of the short-range order parameters was previously carried out only for alloys with the FCC structure [13–16]; for BCC alloys such data are not available.

The goal of the present work is experimental determination of the concentration dependences of the short-range order parameters and the ordering energy of Fe–Re alloys containing 3, 5, and 7 at % of Re by diffuse X-ray scattering (DXS) and calculation of the hypothetical critical temperature of the order—disorder-type phase transition in these alloys in order to identify the type of ordering. According to the state diagram of the Fe–Re system [17], the maximum solubility of rhenium at a temperature of 500°C is approximately 10 at % (Fig. 1). This is taken into account when selecting the compositions for the study of the concentration dependences of the characteristics under consideration. It is seen from Fig. 1 that in the investigated concentration range, there is no ordered structure at temperatures above 400°C.

EXPERIMENTAL PROCEDURE AND CALCULATION OF THE SHORT-RANGE ORDER PARAMETERS AND ELASTIC CONSTANTS

Alloys were prepared from pure charge materials in an atmosphere of pure argon and subjected to repeated melting upon stirring with a magnetic field. The samples were sanded using emery paper with a gradual decrease in the size of abrasive grains and polished with diamond paste to produce a mirror surface. All

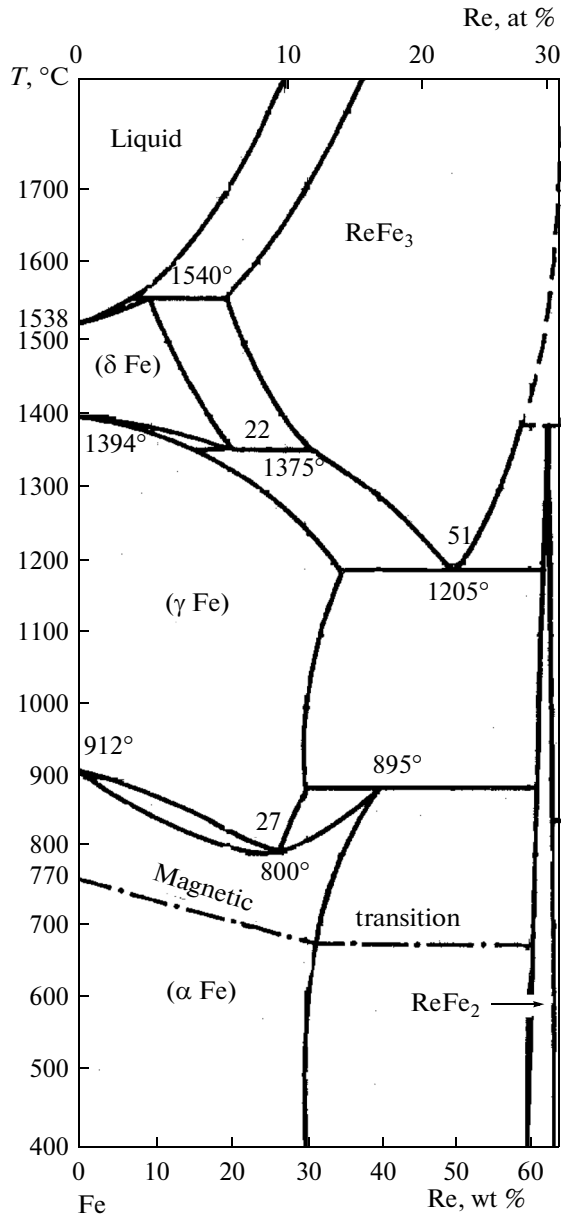

Fig. 1. Phase diagram of the Fe–Re system [17]; there is no ordered structure at temperatures above 400°C in the concentration range of the alloys.

samples were annealed for 3 h at 500°C and quenched in water. After heat treatment, the samples were ground and polished.

The DXS intensity was measured using an X-ray diffractometer with FeK_α radiation and equipped with a flat monochromator Si(111). A BDS-6 scintillation counter with an accuracy of 3–4% was used to record the signals. The intensity of the radiation scattered by the sample was reduced to electronic units by normalizing them to the intensity scattered by fused silica. Then, we subtracted the intensity of scattering in air and Compton and double Bragg scattering from the DXS intensity according to the procedure in [18]. Thereafter, the DXS intensity, minus side effects, is written in the form

$$J(x_j) = nC_AC_B(f_A - f_B)^2 \times \sum_{i=0}^{i_{max}} \alpha_i C_i \left[\frac{\sin q_j r_i}{q_j r_i} + E_i(x_j) + F_i(x_j)\right], \quad (1)$$

where n is the number of atoms in the unit cell; C_A and C_B are the concentrations of alloy components; f_A and f_B are the form-factors of the component atoms, adjusted for anomalous dispersion; $x_j = aq_j/(2\pi)$; $q_j = 4\pi\sin\theta_j/\lambda$; a is the lattice parameter; λ is the X-ray wavelength; θ_j is the scattering angle for the jth data point; α_i and C_i are the short-range order parameter and the coordination number on the ith coordination sphere; and $E_i(x_j)$ and $F_i(x_j)$ are the modulating linear and quadratic functions of the size effect. Modulating functions $E_i(x_j)$ and $F_i(x_j)$ depend on the ratio of elastic moduli C_{12}/C_{11} and C_{44}/C_{11} and the derivative of the concentration $\beta = \frac{1}{V}\frac{\partial V}{\partial C_B}$ as follows:

$$E_i(x_j) = -2[f_A(x_j) - f_B(x_j)]\langle f(x_j)\rangle nC_AC_B\beta I_1(i, x_j),$$
$$F_i(x_j) = \langle f(x_j)\rangle^2 nC_AC_B\beta^2 I_2(i, x_j), \quad (2)$$

where V is the volume of the unit cell; $\langle f(x_j)\rangle = C_Af_A + C_Bf_B$. Function $I_1(i, x_j)$ and $I_2(i, x_j)$ are tabulated for different sets of ratios C_{12}/C_{11} and C_{44}/C_{11} [19].

The values of the elastic constants of iron alloys containing 3, 5, and 7 at % of rhenium are calculated using a model potential [20] through derivation of the pair interatomic potential $V(r)$ according to procedure [21]

$$c_{11} = (6\Omega_0)^{-1}\Sigma'_{l,\alpha}x_\alpha^4(i)\left[\frac{d^2V}{dR^2} - \frac{1}{R}\frac{dV}{dR}\right]_{R=R_i}, \quad (3)$$

$$c_{12} = (6\Omega_0)^{-1}\Sigma'_{l,\alpha\neq\beta}x_\alpha^2(i)x_\beta^2(l)\left[\frac{d^2V}{dR^2} - \frac{1}{R}\frac{dV}{dR}\right]_{R=R_i}, \quad (4)$$

where Ω_0 is the atomic volume; R_i is the radius of the ith coordination sphere; and indices α and β can be 1, 2, or 3: a value of 1 corresponds to the x axis, a value of 2 corresponds to the y axis, and a value of 3 corresponds to the z axis. The projection of an α atom located at the ith coordination sphere on the axis corresponds to the designation $x_\alpha(i)$. The prime mark near the summation sign means that the term with $i = 0$ is excluded. To calculate the value of elastic constant C_{44}, the following ratio was used [21]:

$$\bar{\omega}^2 = a\frac{(2C_{44} + C_{11})}{M}, \quad (5)$$

where $\bar{\omega}^2$ is the second moment of the phonon frequencies, a is the lattice parameter, and M is the atomic weight. The second moment of the phonon fre-

quencies is expressed in terms of derivatives of the pair potential $V(r)$ as follows [21]:

$$\bar{\omega}^2 = (3M)^{-1}\Sigma_i N_i \left(2\frac{dV}{RdR} + \frac{d^2V}{dR^2}\right)_{R=R_i}. \quad (6)$$

Here, N_i is the number of atoms at the ith coordination sphere of radius R_i.

Equations (3), (4), and (6) include the first and second derivatives of the pair interatomic potential $V(r)$, using which we can determine the radial and tangential force constants [22]

$$\alpha_i = \left(\frac{d^2V}{dR^2}\right)_{R_i}; \quad \beta_i = \left(\frac{dV}{RdR}\right)_{R_i}. \quad (7)$$

When calculating the elastic constants of Fe–Re alloys containing 3, 5, and 7 at % of Re, the force constants for rhenium are calculated in the matrix of α-iron. The calculated values of the force constants of α-iron and rhenium are presented in Table 1. The force constants of the alloys are found by averaging the force constants of the components by the concentration

$$\alpha_i^{el} = \sum_{j=1}^{n} \alpha_{ij} c_j; \quad \beta_i^{al} = \sum_{j=1}^{n} \beta_{ij} c_j, \quad (8)$$

where n is the number of alloy components, c_j is the atomic concentration of the jth component, and α_{ij} and β_{ij} are the radial and tangential force constants of the jth component of the multicomponent alloy for the ith coordination sphere.

The calculated elastic constants of α-Fe and Fe–Re alloys containing 3, 5, and 7 at % of Re are given in Table 2. In the same table, the experimental values of the elastic constants of α-Fe [23] are shown for comparison.

Table 1. Power constant of α-iron and rhenium in a matrix of iron, 10^{-3} N/m^{-3}

α-Fe				Re			
α_1	63274.0	β_1	−6956.0	α_1	461452.7	β_1	−67507.0
α_2	15090.0	β_2	−1608.0	α_2	240034.5	β_2	−13643.5
α_3	−2234.0	β_3	237.5	α_3	23131.7	β_3	−1505.6
α_4	−5.4	β_4	−62.8	α_4	−19863.3	β_4	824.9
α_5	894.4	β_5	−38.8	α_5	−21092.0	β_5	−158.0
α_6	−541.1	β_6	31.0	α_6	8872.0	β_6	367.9
α_7	−299.2	β_7	−22.5	α_7	−10709.9	β_7	−49.8
α_8	71.5	β_8	−24.4	α_8	−5329.2	β_8	−264.1
α_9	278.6	β_9	10.3	α_9	5191.8	β_9	152.2
α_{10}	−295.9	β_{10}	7.8	α_{10}	−6296.8	β_{10}	53.9

Table 2. Elastic constants of α-Fe and Fe–Re alloys containing 3, 5, and 7 at % of Re, calculated according to [21], and the experimental data of α-Fe [23]

Alloy	Elastic constants, 10^{10} N/m^2		
	C_{11}	C_{12}	C_{44}
a-Fe	24.8	15.2	12.9
α-Fe (exp.)	24.4	13.8	12.2
Fe–3 at % Re	24.9	15.2	12.8
Fe–5 at % Re	24.1	14.7	12.2
Fe–7 at % Re	23.3	14.1	12.1

EXPERIMENTAL

The experimental DXS intensity values for the alloys containing 3, 5, and 7 at % of rhenium, expressed in electronic units, are presented in Fig. 2 by, respectively, circles, squares, and triangles. It is evident that the dependences of the scattering intensity of alloys on angle 2θ have no obvious diffuse peaks characteristic of solid solutions of the Cu–Au type. For example, for alloys containing 3 and 5 at % of rhenium, a drop in intensity is observed in the range of angles of 10°–16°, and with angles increasing from 16° to 48°, the intensity values increase. In the second range of angles up to 68°, the intensity values fall for all three alloys. We also note that in the alloy with 3 at % of rhenium, the DXS modulation is weaker than in the alloys of other compositions.

Numerical calculations of the short-range order parameters were conducted using the least-squares method. Since the short-range order parameters determined from DXS depend on the concentrations of the components, the Debye temperature T_D, and the statistical shift parameter β, we varied these parameters by the procedure described in [11] for each alloy in order to identify the amount of the minimum sum of the mean square deviations of the theoretical curve from the experimental data (Fig. 2). The calculated values of the short-range order parameters for the first four coordination spheres of iron alloys containing 3, 5, and 7 at % of rhenium, are listed in Table 3. It is seen that for all three alloys, the short-range order parameters for the first coordination sphere are negative. This suggests the existence of short-range order in solid solutions of iron–rhenium. It should be noted

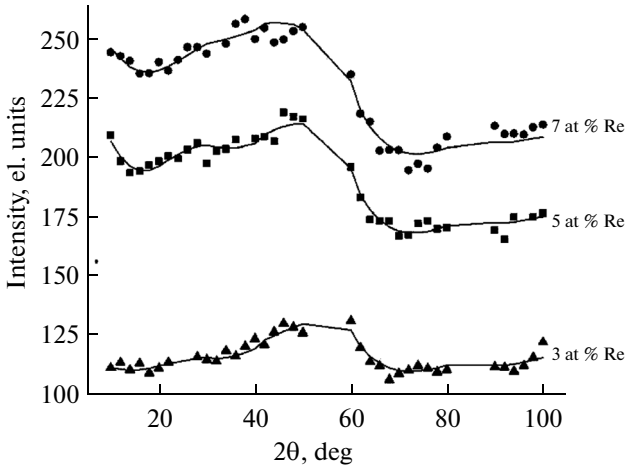

Fig. 2. Experimental values and calculated DXS-intensity curves for Fe–Re alloys: (▲) Fe–3 at % Re, (■) Fe–5 at % Re, and (●) Fe–7 at % Re.

that with the rhenium concentration increasing from 3 to 7 at %, parameter α_1 increases more than twofold. The values of parameter α_2 also grow. It is also seen that for the alloys containing 3 and 5 at % of rhenium, the values of parameter α_3 are negative, and at 7 at % of rhenium, this parameter changes its sign. For all the alloys, the values of parameter α_4 are positive. In the alloys with 3 and 5 at % of rhenium, there is the alternation of signs of the parameters of short-range order, and in the alloy with 7 at % of rhenium, the short-range order parameters for the second, third, and fourth coordination spheres are positive. All of this suggests the strong concentration dependence of the short-range order parameters in solid solutions of iron–rhenium.

The reliability of the results is verified by the data of Fig. 2: the curves of the DXS intensity plotted using the calculated values of the short-range order parameters well describe the experimental data.

CALCULATION OF THE ORDERING ENERGY AND THE CRITICAL TEMPERATURE OF THE ORDER–DISORDER PHASE TRANSITION

Within statistical theory of short-range order by the method of a self-consistent Cowley field [14], we obtained an expression relating the short-range order parameters with the ordering energy

$$-2\Sigma_{n'}\alpha_n V_{nn'} - k_B T \ln\left\{1 + \frac{\alpha_n}{c_A c_B (1-\alpha_n)^2}\right\} = 0, \qquad (9)$$

where α_n is the short-range order parameter at the nth lattice site with respect to the central atom; $\alpha_{n'}$ is the short-range order parameter at the n'th lattice counted from the nth site; $V_{nn'} = (V_{nn'}^{AA} + V_{nn'}^{BB})/2 - V_{nn'}^{AB}$ is the ordering energy at the n'th lattice site also counted from the nth site; $V_{nn'}^{AA}$, $V_{nn'}^{BB}$, $V_{nn'}^{AB}$ are the pair energies of the interactions of atoms A and B; k_B is the Boltzmann constant, c_A and c_B are the atomic concentrations of the alloy components; and T is the absolute temperature.

The calculation of the energy of alloy ordering was carried out using Eqs. (9), which were recorded for the first four coordination spheres as

$$\ln\left\{1 + \frac{\alpha_1}{c_A c_B (1-\alpha_1)}\right\} = -\frac{2}{k_B T}\{(1 + 3\alpha_2 + 3\alpha_3 + \alpha_5)W_1 + (3\alpha_1 + 3\alpha_4)W_2 + (3\alpha_1 + 6\alpha_4 + 3\alpha_7)W_3 + (3\alpha_2 + 6\alpha_3 + 3\alpha_5 + 3\alpha_6 + 6\alpha_8 + 3\alpha_9)W_4\};$$

Table 3. Radii of coordination spheres, short-range order parameters, and ordering energy of Fe–Re alloys

No. of coord. sphere	Fe–3 at % Re			Fe–5 at % Re			Fe–7 at % Re		
	r, Å	α_i	V, k_B	r, Å	α_i	V, k_B	r, Å	α_i	V, k_B
1	2.491	–0.014	228.4	2.495	–0.022	208.6	2.499	–0.039	264.9
2	2.877	0.025	–261.5	2.881	0.028	–187.0	2.886	0.044	–185.1
3	4.068	–0.007	120.6	4.074	–0.005	54.1	4.081	0.000	29.6
4	4.770	0.006	–70.0	4.778	0.008	–62.3	4.785	0.003	–30.6

$$\ln\left\{1+\frac{\alpha_2}{c_A c_B(1-\alpha_2)}\right\} = -\frac{2}{k_B T}\{(4\alpha_1+4\alpha_4)W_1 + (1+4\alpha_3+\alpha_6)W_2 + (4\alpha_2+4\alpha_5+4\alpha_8)W_3 + (4\alpha_1+8\alpha_4+8\alpha_7+4\alpha_{11})W_4\};$$

$$\ln\left\{1+\frac{\alpha_3}{c_A c_B(1-\alpha_3)}\right\} = -\frac{2}{k_B T}\{(2\alpha_1+4\alpha_4+2\alpha_7)W_1 + (2\alpha_2+2\alpha_5+2\alpha_8)W_2 + (1+4\alpha_3+2\alpha_6+4\alpha_9+\alpha_{12})W_3 + (4\alpha_1+6\alpha_4+4\alpha_7+4\alpha_{11}+2\alpha_{10}+4\alpha_{13})W_4\}; \quad (10)$$

$$\ln\left\{1+\frac{\alpha_4}{c_A c_B(1-\alpha_4)}\right\} = -\frac{2}{k_B T}\{(\alpha_2+2\alpha_3+\alpha_5+\alpha_6+2\alpha_8+\alpha_9)W_1 + (\alpha_1+2\alpha_4+2\alpha_7+\alpha_{11})W_2 + (2\alpha_1+3\alpha_4+2\alpha_7+\alpha_{10}+2\alpha_{11}+2\alpha_{13})W_3 + (1+2\alpha_2+3\alpha_3+2\alpha_5+4\alpha_8 + 4\alpha_9+2\alpha_{12}+2\alpha_{14}+\alpha_{15}+2\alpha_{16}+\alpha_{18})W_4\}.$$

The system of linear equations was solved with the experimentally determined parameters of short-range order for the first four coordination spheres by the least-squares method according to the procedure in [16]. The calculated spectra of the ordering energy of the alloys are given in units of the Boltzmann constant k_B in Table 3. It can be concluded from the table that for all the alloys, the values of the ordering energy alternately change sign with increasing number of the coordination sphere. Moreover, for the alloys containing 3 and 5 at % of rhenium, alternation of the sign of the ordering energy coincides with alternating sign of the short-range order parameters. The unit value of the ordering energy for the second, third, and fourth spheres decreases with increasing concentration of rhenium. For the Fe–3 at % Re alloy, the value of the ordering energy for the second coordination sphere exceeds in absolute magnitude the value for the first sphere. For the Fe–7 at % Re alloy, the module of the ordering energy decreases with increasing number of the coordination sphere. For this alloy, the value of the ordering energy under the first field is higher than that for alloys Fe–3 and 5 at % Re by 16 and 27%, respectively. The ordering energies of the iron alloys containing 3, 5, and 7 at % of rhenium were approximated by the dependences of the ordering energy on the interatomic distances using third-degree polynomials. The graphs are shown in Fig. 3; it is seen that the dependences of the ordering energy of alloys Fe–3, 5, and 7 at % Re on the interatomic distance have an oscillating character. The oscillating nature of the ordering energy on the interatomic distance was also found in Cu_3Au [15] and Ni_3Al [16] alloys.

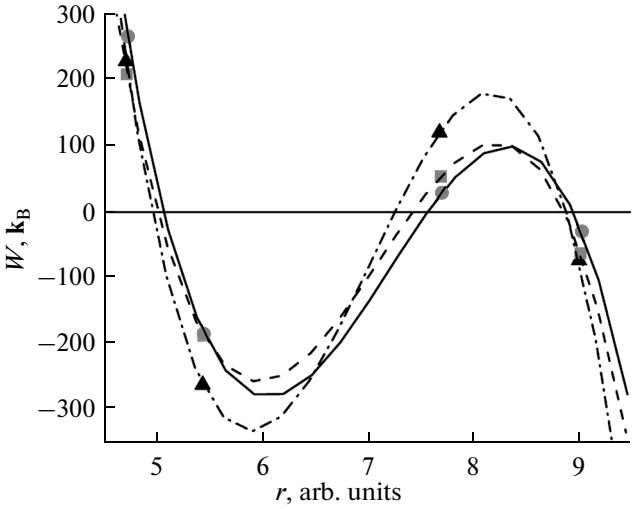

Fig. 3. Dependence of the ordering energy of alloys Fe–3, 5, and 7 at % Re on the interatomic distance: (▲) Fe–3 at % Re, (■) Fe–5 at % Re, and (●) Fe–7 at % Re.

Using the values of the ordering energy and the short-range order parameters, the energy of the short-range order for each alloy was calculated by equation

$$E_{SR} = \Sigma_i c_i \alpha_i W_i, \quad (11)$$

where c_i is the coordination number for the ith coordination sphere, α_i is the short-range order parameter, and W_i is the ordering energy for the ith coordination sphere. The values of the short-range order energy for the alloys containing 3, 5, and 7 at % of rhenium are respectively −85.4, −77.3, and −133.7 k_B, which leads to the conclusion that in the alloy of Fe–7 at % Re, short-range ordering plays the most stabilizing role. In order to confirm this fact, we calculated the hypothetical critical temperature of the order–disorder-type phase transition for the alloys.

According to Cowley [13], the expression for the critical temperature can be deduced from the second equation of system (10) with limiting values of the

Table 4. Limiting values of parameters α_i for some superstructures

i	B2	DO_3	B32
1	−1	−1/3	0
2	1	−1/3	−1
3	1	1	1
4	−1	−1/3	0
5	1	−1/3	−1
6	1	1	1
7	−1	−1/3	0
8	1	−1/3	−1

Table 5. Hypothetical critical temperature of the Fe–Re alloys for three types of superstructures

Alloy	Type of superstructure		
	B2	DO_3	B32
Fe–3 at % Re	11.5 K	120.0 K	175.5 K
Fe–5 at % Re	61.4 K	132.6 K	168.3 K
Fe–7 at % Re	278.9 K	220.1 K	194.8 K

short-range order parameters corresponding to a specific superstructure. These limiting values for BCC superstructures B2 and DO_3 are given in Table 4 according to [1]. By substituting the limiting values for the short-range order parameters for a B2 superstructure in the second equation of system (10) and by performing subsequent transformations, we obtain an expression for the critical temperature

$$T_c = -\frac{2c_A c_B}{k_B}\left[-8W_1 + 6W_2 + 12W_3 - 24W_4\right]. \quad (12)$$

We can obtain the same equation, according to [24], from the expression relating the Fourier transform of the spectrum of short-range order parameter $\alpha(\mathbf{k})$ and the Fourier transform of the spectrum of ordering energy $W(\mathbf{k})$

$$\alpha(\mathbf{k}) = -\frac{c}{[1 + 2c_A c_B(1/k_B T)W(\mathbf{k})]}, \quad (13)$$

where T is the temperature of alloy quenching, and C is the normalization constant. According to [24], the absolute minimum of $W(\mathbf{k})$ is achieved at points of reciprocal space, where $\alpha(\mathbf{k})$ has the maximum value for a disordered phase. The critical point can be defined as the temperature, at which the denominator of Eq. (13) approaches zero at the corresponding point of the reciprocal lattice. Therefore, critical temperature T_c is determined from equation

$$1 = -2c_A c_B(1/k_B T_c)W(\mathbf{k_m}), \quad (14)$$

where $W(\mathbf{k_m})$ is the value of $W(\mathbf{k})$ at the point on the reciprocal lattice, where it has the absolute minimum. For a B2 superstructure, there is a minimum of $W(\mathbf{k})$ at points $\mathbf{k_m}(1,0,0)$ and $\mathbf{k_m}(1,1,1)$.

The expression for the Fourier transform of $W(\mathbf{k})$ is [24]

$$W(\mathbf{k}) = \Sigma_{lmn} W_{lmn} \cos \pi l h_1 \cos \pi m h_2 \cos \pi n h_3, \quad (15)$$

wherein $\mathbf{k} = h_1\mathbf{b}_1 + h_3\mathbf{b}_2 + h_3\mathbf{b}_3$, (h_1, h_2, h_3) are the coordinates of a point on the reciprocal lattice; $\mathbf{b}_1$, $\mathbf{b}_2$, and $\mathbf{b}_3$ are the reciprocal-lattice vectors; (l, m, n) are the coordinates of the lattice selected in such a way that the radius vector of the site is designated as $\mathbf{r}(lmn) = (l\mathbf{a}_1 + m\mathbf{a}_2 + n\mathbf{a}_3)/2$. Thus, $\mathbf{a}_1$, $\mathbf{a}_2$, and $\mathbf{a}_3$ are the fundamental translations of a cubic lattice, and integers l, m, and n for the BCC lattice are numbers of the same parity. At the points of reciprocal space $\mathbf{k_m}(1,0,0)$ and $\mathbf{k_m}(1,1,1)$, the Fourier transform (Eq. (15)) is

$$W(\mathbf{k_m}) = -8W_1 + 6W_2 + 12W_3 - 24W_4. \quad (16)$$

From Eqs. (14) and (16), we can derive expression (12).

Using the calculated values of the ordering energy for the first four coordination spheres and the limiting parameters for short-range order for a B2 superstructure, listed in Table 4, we calculated the hypothetical values of the critical temperature T_c of the order–disorder phase transition for the alloys under study according to Eq. (12); the results are presented in Table 5.

Another possible BCC superstructure is DO_3, the limiting short-range order parameters for which are shown in Table 4 [1]. For this superstructure, an equation for the critical temperature T_c was obtained from Eq. (11), that is,

$$T_c = -\frac{2c_A c_B}{k_B}\left[-\frac{8}{3}W_1 + 6W_2 - 4W_3 - 8W_4\right]. \quad (17)$$

The results of calculations in accordance with Eq. (17) are presented in Table 5; it is seen that the highest hypothetical temperature of a phase transition of the order–disorder type is observed for the Fe–7 at % Re alloy.

According to [24], a B32 superstructure is included in the BCC lattice, for which there is a minimum of $W(\mathbf{k_m})$ at point $\mathbf{k_m}(1/2, 1/2, 1/2)$,

$$W(\mathbf{k_m}) = -6W_2 + 12W_3.$$

Therefore, the expression for the critical temperature with respect to the B32 superstructure is

$$T_c = -\frac{2c_A c_B}{k_B}\left[-6W_2 + 12W_3\right]. \quad (18)$$

Meanwhile, we can obtain the following equation from the Cowley formula:

$$T_c = -\frac{2c_A c_B}{k_B}\{(4\alpha_1 + 4\alpha_4)W_1 + (1 + 4\alpha_3 + \alpha_6)W_2 + (4\alpha_2 + 4\alpha_5 + 4\alpha_8)W_3 + (4\alpha_1 + 8\alpha_4 + 8\alpha_7 + 4\alpha_{11})W_4\}. \quad (19)$$

From comparison of Eqs. (18) and (19) for specific crystalline structures, the limiting values for the short-range order parameters were derived for a B32 superstructure, which are given in Table 4. The results of calculation of the hypothetical critical temperature of the alloys under study for a B32 superstructure are shown in Table 5; it is demonstrated that for the B32 and DO_3 superstructures, the hypothetical critical temperature in the iron alloys containing 3, 5, and 7 at % of rhenium increases with increasing concentration of rhenium. For all considered structures, the hypothetical temperature is below room temperature, which is

due to weak short-range order in the alloys and is consistent with the phase diagram of the Fe–Re system (Fig. 1). The highest hypothetical critical temperature is obtained for the Fe–7 at % Re alloy, which is consistent with the above results of calculation of the short-range order energy. For this alloy, according to the range of the experimental values of the parameters of short-range order for the first four coordination spheres and the data of Table 4, it can be concluded that the short-range ordering tends to the B3 superstructure. For all three alloys, the critical temperature calculated for the B3 superstructure exceeds the temperature values corresponding to the other two types of superstructures.

CONCLUSIONS

Based on data on the DXS intensity, the concentration dependence of the short-range order parameters of Fe–Re alloys is experimentally found. Using spectra of the short-range order parameter obtained by the Cowley equations, written for the first four coordination spheres of a BCC lattice, we calculated the values of the ordering energy for the first four coordination spheres of iron alloys containing 3, 5, and 7 at % of rhenium and found an oscillating dependence of the ordering energy on the interatomic distance for all these alloys. We derived expressions for calculation of the critical temperature for the order–disorder transition for BCC superstructures B3, B32, and DO_3, using which we established the tendency of the Fe–7 at % Re alloy to ordering according to the B3 type. For this alloy, the short-range order energy exceeds in absolute value the energies of short-range order, corresponding to alloys containing 3 and 5 at % of rhenium.

ACKNOWLEDGMENTS

The work was supported by the project of the Mongolian State University "Study of the Crystal Lattice Dynamics, Magnetic and Optical Properties, and Ordering Processes."

REFERENCES

1. V. I. Iveronova and A. A. Katsnelson, *Short-Range Order in Solid Solutions* (Nauka, Moscow, 1977) [in Russian].
2. V. M. Silonov, Radioelektron., Nanosist., Inform. Tekhnol., No. 31, 34 (2011).
3. V. A. Tatarenko and T. M. Radchenko, Usp. Fiz. Met., No. 3, 111 (2002).
4. E. N. Vlasova, Fiz. Met. Metalloved. **16**, 355 (1963).
5. E. N. Vlasova and V. I. Iveronova, Sov. Phys. Solid State **15**, 176 (1963).
6. V. I. Iveronova and A. A. Katsnelson, Fiz. Met. Metalloved. **19**, 696 (1965).
7. C. R. Houska and B. L. Averbach, J. Phys. Chem. Solids **23**, 1763 (1962).
8. V. I. Iveronova, A. I. Minaev, and V. M. Silonov, Fiz. Met. Metalloved. **33**, 978 (1972).
9. T. Ericsson and J. B. Cohen, Acta Crystallogr. A **27**, 97 (1971).
10. A. A. Katsnelson, V. M. Silonov, and Abu Al Shamlat Salama, Vestn. Mosk. Univ., Fiz. Astron., No. 35, 66 (1994).
11. V. M. Silonov and L. Enkhtor, Izv. Vyssh. Uchebn. Zaved., Fiz., No. 3, 71 (1998).
12. V. M. Silonov and L. Enkhtor, Vestn. Mosk. Univ., Fiz. Astron., No. 3, 37 (1997).
13. J. M. Cowley, Phys. Rev. **77**, 669 (1950).
14. S. C. Moss and P. C. Clapp, Phys. Rev. **171**, 764 (1968).
15. S. Wilkins, Phys. Rev. B **2**, 3935 (1970).
16. A. A. Katsnelson and P. Sh. Dazhaev, Fiz. Met. Metalloved. **37**, 625 (1974).
17. *State Diagrams of Binary Metallic Systems*, Ed. by N. P. Lyakishev (Moscow, Mashinostroenie, 1997) [in Russian].
18. V. M. Silonov and L. Enkhtor, Fiz. Met. Metalloved. **80** (5), 79 (1995).
19. A. A. Katsnelson, O. V. Kris'ko, V. M. Silonov, and T. V. Skorobogatova, Available from VINITI No. 4751 (MSU, Moscow, 1983).
20. A. O. E. Animalu, Phys. Rev. B **8**, 3542 (1973).
21. G. Leibfried, *Handbuch der Physik*, part 1, vol. 7: *Gitterthoerie der mechanisohen und thermoschen Eidenschaften der Kristalle* (Springer, Berlin, 1955) [in German].
22. W. M. Shyu and G. D. Gaspari, Phys. Rev. **170**, 687 (1968).
23. Landolt–Börnstein, *Numerical Data and Function Relationships in Science and Technology*, New Series, Group III: *Condensed Matter* (Springer, Berlin, Heidelberg, 1983), vol. 18.
24. S. C. Moss and P. C. Clapp, Phys. Rev. **171**, 754 (1968).

Translated by O. Zhukova